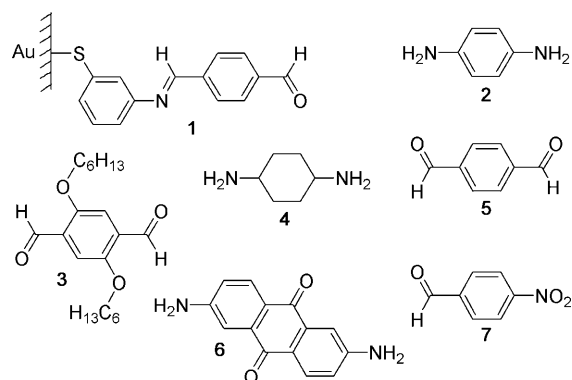


# In Situ Stepwise Synthesis of Functional Multijunction Molecular Wires on Gold Electrodes and Gold Nanoparticles\*\*

Geoffrey J. Ashwell,\* Barbara Urasinska-Wojcik, and Laurie J. Phillips

Interest in molecular electronics has focused on materials that act as diodes<sup>[1,2]</sup> or wires,<sup>[3–5]</sup> and on the development of innovative techniques for contacting to single molecules and ultrathin films.<sup>[6–14]</sup> They include, for example, the in situ synthesis of molecular wires on solid supports,<sup>[10–14]</sup> in which recent advances have resulted in the bridging of nanometer-sized gaps between electrodes by the coupling of amino-terminated molecules between opposing surface-based aldehyde groups on the electrode coatings.<sup>[12–14]</sup> For photovoltaic applications, molecules may be elongated in situ on nanoparticles with differently colored linked units to provide charge-transport pathways along the conjugated wirelike backbones.<sup>[15]</sup> This elongation method is highly versatile: it combines a facile synthesis, user-defined functionality during the initial self-assembly of the precursors to provide reactive surface-based groups, and the sequencing of chemical building blocks (donors, acceptors, and bridges) to match the energy levels with those of the electrodes. The current–voltage (*I*–*V*) characteristics, which are usually symmetrical for conventional wires, may be tuned by controlling the molecular sequence. Donors and acceptors give rise to rectifying characteristics when isolated at opposite ends and the direction of electron flow at forward bias is from the cathode to acceptor on one side and from the donor to anode on the other. Improved rectification has been achieved by incorporating a cyclohexane  $\sigma$  bridge that inhibits intramolecular charge transfer and maintains the integrity of the electron-donating and electron-accepting moieties. This additional bridge has resulted in the highest rectification ratio to date from a molecular diode.

Molecular wires were synthesized in situ on gold electrodes from a self-assembly reaction of a *meta*-substituted thiophenol with a terminal aldehyde group to act as a template for growth that is perpendicular to the substrate (Figure 1). These embryonic wires were elongated by reacting first with H<sub>2</sub>N-wire-NH<sub>2</sub> and then OHC-wire-CHO to couple the wire-like units through imino groups. The sequence is



**Figure 1.** Structure of the self-assembled monolayer (SAM), which was obtained from 4-[(3-mercaptophenylimino)methyl]benzaldehyde precursor **1**, and aldehyde and amine substrates that were used for in situ elongation of the wire.

user-defined and the wires may be elongated to any appropriate length by repeating the process before terminating with a mono-substituted component. In this study, plasma-cleaned substrates were immersed in a solution of 4-[(3-mercaptophenylimino)methyl]benzaldehyde in acetone (0.1 mg cm<sup>-3</sup>, step 1) for 4 h and then rinsed with acetone to remove physisorbed material. When assembled on the electrodes of 10 MHz quartz crystals, a Sauerbray analysis<sup>[16]</sup> of the limiting frequency change gave an area of 0.3 nm<sup>2</sup> molecule<sup>-1</sup>, which approximates to the molecular cross-section. Chemisorption was verified by X-ray photoelectron spectroscopy (XPS): a doublet at 162.1 eV (S 2p<sub>3/2</sub>) and 163.3 eV (S 2p<sub>1/2</sub>) is characteristic of the Au–S link, and a peak at 399.1 eV (N 1s) corresponds to the imino nitrogen atom. Quantitative analysis of the areas under the S 2p and N 1s peaks, which was fitted using a Gaussian-Lorentzian function and corrected for atomic sensitivity factors, confirmed an N:S ratio of about 1:1, consistent with the atomic ratio within the self-assembled molecule.

Mercaptoaniline (HS–C<sub>6</sub>H<sub>4</sub>–NH<sub>2</sub>)<sup>[17]</sup> binds to the gold surface through both the nitrogen and sulfur substituents, as shown by the characteristic XPS data of each bond: 162.0 and 163.2 eV (S 2p, Au–S); 163.6 and 164.8 eV (S 2p, SH); 398.3 eV (N 1s, Au–N); 400.4 eV (N 1s, NH<sub>2</sub>). As such, 4-[(3-mercaptophenylimino)methyl]benzaldehyde **1** was chosen as the starting building block for the molecular wires (Figure 1). However, mercaptoaniline was used in a preliminary study to demonstrate the in situ growth of molecular wires on gold nanoparticles. When functionalized by 3-mercaptoaniline, these nanoparticles exhibited NH<sub>2</sub> IR absorption stretching modes at 3200 and 3300 cm<sup>-1</sup>, but subsequent reaction with terephthalaldehyde resulted in the loss of them and the

[\*] Prof. G. J. Ashwell,<sup>[†]</sup> Dr. B. Urasinska-Wojcik, L. J. Phillips  
College of Physical and Applied Sciences, Bangor University  
Bangor, Gwynedd LL57 2UW (UK)

[†] Current address: Physics Department, Lancaster University  
Lancaster LA1 4YB (UK)  
E-mail: g.j.ashwell@lancaster.ac.uk

[\*\*] We thank the EPSRC, Technology Strategy Board, and the EC FP7 ITN “FUNMOLS” project no. 212942 for financial support, Prof. Ian Gentle for access to the XPS facility at the University of Queensland, and Piotr Wierzchowicz and Kym Ford for technical assistance.

Supporting information for this article is available on the WWW under <http://dx.doi.org/10.1002/anie.200906607>.

formation of stretching modes at  $1609\text{ cm}^{-1}$  (C=N) and  $1703\text{ cm}^{-1}$  (C=O; Figure 2). The latter stretches were quenched by reaction with amino-substituted units, and their appearance and disappearance is consistent with the

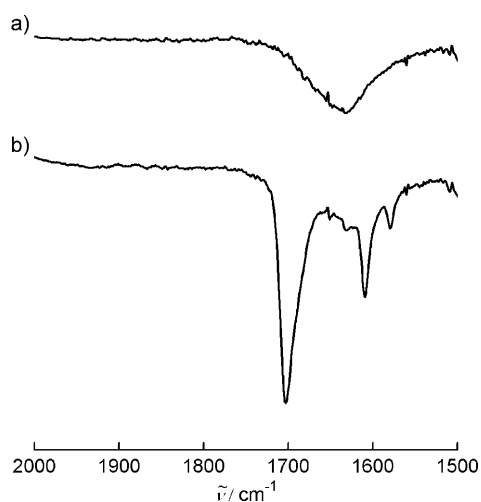


**Figure 2.** IR spectra: a) self-assembled 3-mercaptoaniline monolayers on gold nanoparticles and b) evolution of peaks at  $1609\text{ cm}^{-1}$  (C=N) and  $1703\text{ cm}^{-1}$  (C=O) following reaction with 5.

formation of imino links between the reacted units. As part of an extended study, the analogous in situ coupling reaction has been demonstrated for platinum and silver nanoparticles that were functionalized by 3-mercaptoaniline and  $\text{TiO}_2$  nanoparticles treated with 4-aminobenzoic acid.

The in situ growth of embryonic molecular wires on planar substrates was performed at ambient temperature by the initial self-assembly of 4-[(3-mercapto-phenylimino)methyl]-benzaldehyde on, for example, the gold electrodes of 10 MHz quartz crystals, and thereafter, by immersing the SAM-coated (SAM = self assembled monolayer) substrates in solutions of each of the following reactants (1 mg in  $10\text{ cm}^3$ ;  $0.05\text{ cm}^3$  glacial acetic acid was added in each case): 1,4-phenylenediamine **2** in acetone (step 2); 2,5-bis(hexyloxy)-terephthalaldehyde **3** in acetone (step 3); 1,4-diaminocyclohexane **4** in methanol (step 4); terephthalaldehyde **5** in tetrahydrofuran (step 5); 2,6-diaminoanthra-9,10-quinone **6** in tetrahydrofuran (step 6); and 4-nitrobenzaldehyde **7** in acetone (step 7). The monolayer was immersed in each solution for 2–3 hours and rinsed with the appropriate solvent to remove any physisorbed material. Coupling was indicated by a stepwise decrease in the frequency of the quartz crystals, and the condensation was verified by XPS data that are consistent with the formation of imino links (Table 1). For example, the N 1s core-level spectrum of the initially formed SAM was altered following reaction with 1,4-phenylenediamine, and exhibited peaks at 399.3 and 400.6 eV with an area ratio of about 2:1 (Figure 3). Those peaks corresponded to imino and amino groups, respectively, and, when corrected for atomic sensitivity factors, their combined area relative to sulfur was about 3:1 (cf. 1:1 for the SAM).

**Table 1:** XPS data: sulfur (S  $2p_{3/2}$  and S  $2p_{1/2}$ ) and nitrogen (N 1s) binding energies (B.E.s) for each stage of the seven step process.

Step	B.E. [eV] (Au-S)	B.E. [eV] (CH=N)	B.E. [eV] (NH <sub>2</sub> )	B.E. [eV] (NO <sub>2</sub> )
1	162.1, 163.3	399.1	–	–
2	162.0, 163.2	399.3	400.6	–
3	162.2, 163.4	399.2	400.7	–
4	162.3, 163.5	399.3	400.8	–
5	162.0, 163.2	399.3	400.9	–
6	162.0, 163.2	399.2	400.7	–
7	162.1, 163.3	399.1	400.9	405.0

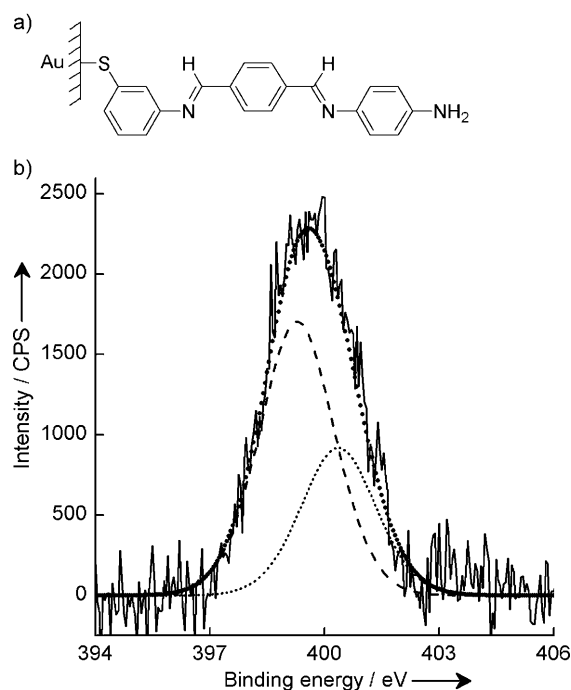


**Figure 3.** Molecular structure of the embryonic wire following step 2 and its deconvoluted N 1s core-level spectrum. The 2:1 area ratio of the peaks at 399.3 and 400.6 eV from the imine and amine, respectively, is consistent with the ratio in the molecule.

Analytical data for each stage of the stepwise elongation are included in the Supporting Information; quartz crystal and XPS data for the rectifying wire, which was formed in seven steps, are depicted in Figure 4. These data suggest a quantitative reaction except in the third step where the bulky  $\text{C}_6\text{H}_{13}\text{O}$  substituents of 2,5-bis(hexyloxy)terephthalaldehyde restricted the coupling yield to 50%. This conclusion is confirmed from the plot of frequency change versus relative molecular mass of the stepwise elongated wire in which the initial slope, steps 1 and 2, is double that of steps 3 to 7 (Figure 4b). XPS studies also showed that the N:S ratios obtained for steps 4 to 7 are consistent with  $(50 \pm 10)\%$  coupling at step 3 (Figure 4c). Discrepancies may arise from using different depth profiles; therefore, XPS studies were performed at a takeoff angle of  $45^\circ$  to minimize the influence of sulfur being bonded to the substrate when the nitrogen atoms are located throughout the film. However, both XPS and the quartz crystal analyses indicate that the steric bulk of

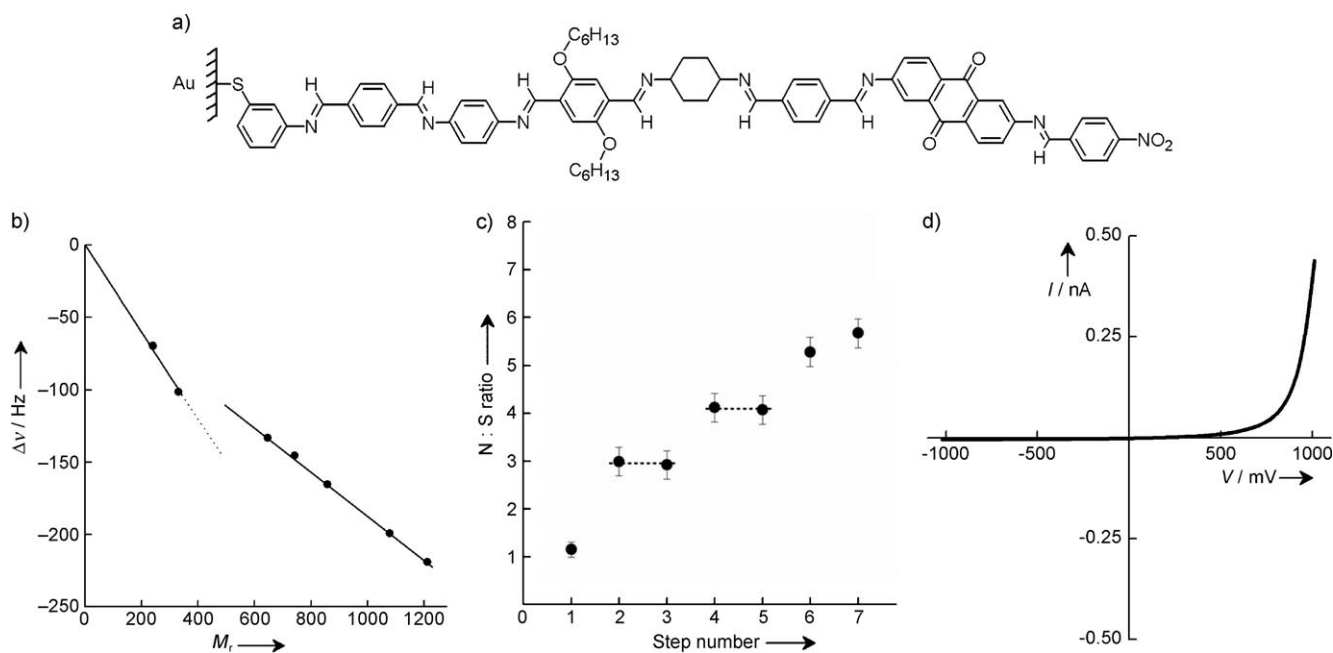


**Figure 4.** Multijunction molecular wire: a) Molecular structure of the wire that was synthesized by the stepwise in situ coupling of seven components on a gold electrode. b) Frequency change versus relative molecular mass ( $M_r$ ) for the self-assembly of embryonic wires at the gold electrodes of 10 MHz quartz crystals and its subsequent elongation in six steps. c) N:S ratios that were calculated from the peak areas of the N 1s and S 2p core-level spectra, corrected for atomic sensitivity factors; steps 3 and 5 showed no increase in the ratio as the terephthalaldehyde linking units do not contain nitrogen. d)  $I$ - $V$  characteristics obtained using a set point current of 600 pA and a voltage of 80 mV. The sign corresponds to the substrate electrode; at a forward bias (positive quadrant), electrons tunnel from the gold probe to the gold-coated substrate.

the alkyloxy side chains hindered the third step of the reaction and that, thereafter, the coupling reactions proceed stoichiometrically in solution with exposed surface-active groups.

The deconvoluted sulfur spectrum for the final step of the chain elongation process had characteristic gold thiolate XPS peaks at 162.1 eV (S 2p<sub>3/2</sub>) and 163.3 eV (S 2p<sub>1/2</sub>) with an expected peak separation of 1.2 eV and area ratio of 2:1. The deconvoluted nitrogen spectrum revealed peaks at 399.1 (strong), 400.9 (weak), and 405.0 eV (weak), which correspond to the imino links, and the amino and nitro groups respectively. No amino groups were present in the nitro-terminated wire (Figure 4a); instead, the weak peak at 400.9 eV related to the amino substituent on the embryonic wire, shown in Figure 2, whose growth was inhibited by the bulky hexyloxy ring-substituted reactant for the next step. Following the final elongation step, the wire had a 50% occupancy and an experimental N:S ratio of ( $5.7 \pm 0.3$ ), which was consistent with a mean of 5.5 for the short (3:1) and long (8:1) wires formed in steps 2 and 7, respectively.

The  $I$ - $V$  characteristics of the nitro-group-terminated wire were studied by STM (scanning tunneling microscopy) at different locations across the films and, using contacting gold probes, the data were averaged from multiple scans on the same spot. The profile was found to be independent of the set point current and the voltage, which affect the magnitude of the current by altering the distance between the probe and the surface but have minimal effect on the shape of the  $I$ - $V$  curves of the rectifying molecule. A slight asymmetry could be induced in the shape of the  $I$ - $V$  curve by varying the set point conditions but, for example, the maximum current ratio from

$I$ - $V$  curves of symmetrical molecules is typically less than about 5 at  $\pm 1$  V. This value is trivial compared with data obtained for the donor-acceptor structure. The forward bias direction of the electron flow is consistent with the model reported by Aviram and Ratner (Figure 4d).<sup>[1]</sup> It is from the gold probe (cathode) to the lowest unoccupied molecular orbital (LUMO) of the electron-accepting end of the wire on one side, and from the highest occupied molecular orbital (HOMO) of the electron-donating end to the gold substrate (anode) on the opposite side. At reverse bias, a mismatch between the Fermi energies of the electrodes and the energy levels of the conjugated units that are isolated by the  $\sigma$  bridge is responsible for the  $I$ - $V$  characteristics.

The rectification ratio of approximately 160 at  $\pm 1$  V is the highest to date for a molecular diode, although we note that higher values have been obtained from a bilayer structure (an organic rectifying junction).<sup>[18]</sup> The magnitude of this ratio is influenced, in part, by the acceptor arrangement (nitrobenzene and anthraquinone) on one side and electron-donating (hexyloxy) substituents on the other, and also, in part, by the  $\sigma$  bridge. This cyclohexane tunneling barrier plays a pivotal role in improving rectification by, for example, suppressing zero-bias charge transfer and maintaining the integrity of the electron-donating and electron-accepting ends. The ratio may be contrasted with about 20 at  $\pm 1$  V for a  $\pi$ -bridged sequence with the same series of donors and acceptors but no  $\sigma$ -bridged tunneling barrier at step 4. Moreover, the majority of molecular diodes<sup>[19-25]</sup> exhibit slight rectification with ratios in the range 5-30 at  $\pm 1$  V when contacted by non-oxidizable electrodes. There are

exceptions,<sup>[2a]</sup> and high ratios have been reported for bilayer arrangements in which cationic acceptor-( $\pi$ -bridge)-donor structures are ionically coupled to anionic phthalocyanine donors.<sup>[18]</sup> However, the rectification ratio of 160 at  $\pm 1$  V, obtained herein, is by far the highest for a monolayer, and has been achieved by the in situ coupling of the component parts.

In conclusion, we have sequenced electroactive units along the length of a molecular wire and shown that the energy levels on opposite sides may be manipulated to achieve improved rectification by locating a tunneling barrier between the electron-donating and electron-accepting moieties. Difficulties in alignment have inhibited previous studies of donor-( $\sigma$ -bridge)-acceptor diodes,<sup>[26,27]</sup> but they may be readily designed, synthesized, and aligned by in situ growth. This study has resulted in the highest rectification ratio to date for a molecular diode and, as part of our continuing work, the templated sequencing of electroactive moieties on solid supports is being applied to other types of substrates, including silicon. This technique is highly versatile and the sequencing of donors and acceptors as well as electron bridges permits the band structure and absorption characteristics to be finely tuned for electronic and photonic applications.

### Experimental Section

4-[(3-Mercaptophenylimino)methyl]benzaldehyde (**1**), was synthesized from the reaction of 3-mercaptoaniline (0.75 g, 6 mmol) and excess terephthalaldehyde (1.6 g, 12 mmol) in ethanol (50 cm<sup>3</sup>) at ambient temperature. The solvent was removed in vacuo and the pale yellow product was recrystallized from chloroform and acetone and washed with ethanol: 90% yield; m.p. 227 °C; UV (C<sub>2</sub>H<sub>5</sub>OH):  $\lambda_{\text{max}}$  = 340 nm; IR (KBr):  $\tilde{\nu}$  = 1620 cm<sup>-1</sup> (C=N), 1700 cm<sup>-1</sup> (C=O), 2550 cm<sup>-1</sup> (S-H); elemental analysis calcd for C<sub>14</sub>H<sub>11</sub>NOS: C 69.69, H 4.60, N 5.81%; found: C 69.4, H 4.4, N 5.5%; XPS: S 2p<sub>3/2</sub> 164.1 eV, S 2p<sub>1/2</sub> 165.3 eV (SH), C 1s 284.7 eV (C<sub>Ar</sub>), 285.4 eV (C=N), 286.1 eV (C-S), 287.4 eV (C=O), N 1s 399.3 eV (CH=N), O 1s 531.9 eV (C=O); MS *m/z* (%): 241 (100); HRMS, *m/z*: 241.0552 [*M*]<sup>+</sup>, calculated 241.0556.

Functionalized gold nanoparticles were prepared by adapting the method reported by Brust et al.<sup>[28]</sup> Tetraoctylammonium bromide (2.2 g, 4 mmol) in toluene (100 cm<sup>3</sup>) was added to an aqueous solution (100 cm<sup>3</sup>) of gold(III) chloride trihydrate (0.32 g, 0.8 mmol, 50 cm<sup>3</sup>). The mixture was stirred to transfer the auric chloride into the organic phase, to which 3-mercaptoaniline (0.25 g, 2 mmol) and then an aqueous solution of sodium borohydride (0.76 g, 20 mmol, 50 cm<sup>3</sup>) were added with stirring. The organic phase was separated after 16 h, evaporated in vacuo, and the functionalized nanoparticles were washed with water (2 × 30 cm<sup>3</sup>) and ethanol (2 × 30 cm<sup>3</sup>). The nanoparticles were then treated with a chloroform solution of terephthalaldehyde (0.40 g, 3 mmol, 50 cm<sup>3</sup>), for 48 h at ambient temperature, filtered, and washed with ethanol. Reaction with the dialdehyde yielded a CO stretch at 1703 cm<sup>-1</sup> and a C=N stretch at 1609 cm<sup>-1</sup>, with loss of the NH<sub>2</sub> stretch at 3200–3300 cm<sup>-1</sup>. The resultant spectrum is consistent with formation of the self-assembled form of 4-[(3-mercaptophenylimino)methyl]benzaldehyde; we note that subsequent reaction with aniline resulted in the loss of the CO stretch, the sequential appearance and disappearance of which is indicative of coupling through imino linkages.

XPS studies were performed on organic layers on gold-coated highly oriented pyrolytic graphite, and on powdered samples of the self-assembling precursor. Spectra were recorded at step intervals of 0.05 eV and acquired for monochromatic Al<sub>K $\alpha$</sub>  radiation using a Kratos Axis Ultra spectrometer, operated at a pressure of  $< 9 \times 10^{-7}$  Pa. Data for each step of the elongated wire and its powdered precursor were referenced to the gold 4f peak at 84.0 eV and carbon

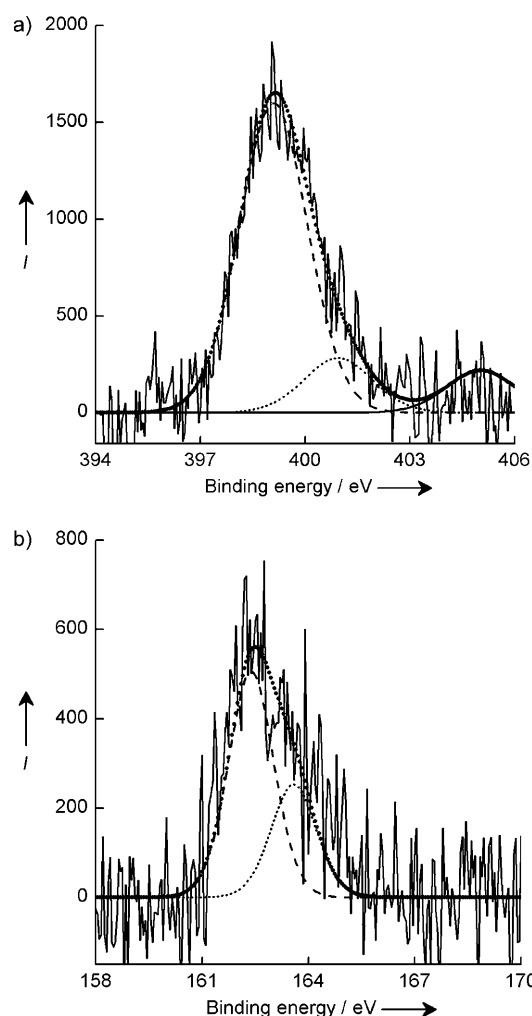


**Figure 5.** Core-level spectra of an elongated wire that was formed in seven steps: a) N 1s, 399.1 eV (C=N), 400.9 eV (NH<sub>2</sub>) and 405.0 eV (NO<sub>2</sub>); b) S 2p, 162.1 and 163.3 eV (Au-S). The weak amino shoulder arises from the embryonic wire formed in step 2 (see text).

1s peak at 284.7 eV respectively and analyzed using Casa XPS software. Spectra for the wire formed from the seventh stage of the in situ process are included in the Supporting Information, and shown in Figure 5.

Received: November 23, 2009

Published online: March 31, 2010

**Keywords:** molecular diodes · molecular electronics · nanotechnology · organic photovoltaics · self-assembly

- [1] A. Aviram, M. A. Ratner, *Chem. Phys. Lett.* **1974**, *29*, 277–283.
- [2] a) G. J. Ashwell, A. Mohib, *J. Am. Chem. Soc.* **2005**, *127*, 16238–16244; b) G. J. Ashwell, W. D. Tyrrell, A. J. Whittam, *J. Am. Chem. Soc.* **2004**, *126*, 7102–7110.
- [3] S. Wu, M. T. Gonzalez, R. Huber, S. Grunder, M. Mayor, C. Schönberger, M. Calame, *Nat. Nanotechnol.* **2008**, *3*, 569–574.
- [4] G. J. Ashwell, B. Urasinska, C. Wang, M. R. Bryce, I. Grace, C. J. Lambert, *Chem. Commun.* **2006**, 4706–4708.
- [5] X. Guo, J. P. Small, J. E. Klare, Y. Wang, M. S. Purewal, I. W. Tam, B. H. Hong, R. Caldwell, L. Huang, S. O'Brien, J. Yan, R.

- Breslow, S. J. Wind, J. Hone, P. Kim, C. Nuckolls, *Science* **2006**, *311*, 356–359.
- [6] L. T. Cai, H. Skulason, J. G. Kushmerick, S. K. Pollack, J. Naciri, R. Shashidar, D. L. Allara, T. E. Mallouk, T. S. Mayer, *J. Phys. Chem. B* **2004**, *108*, 2827–2832.
- [7] J. Reichert, R. Ochs, D. Beckmann, H. B. Weber, M. Mayor, H. v. Löhneysen, *Phys. Rev. Lett.* **2002**, *88*, 176804.
- [8] J. Hihath, N. Tao, *Nanotechnology* **2008**, *19*, 265204.
- [9] S. W. Howell, S. M. Dirk, K. Childs, H. Pang, M. Blain, R. J. Simonson, J. M. Tour, D. R. Wheeler, *Nanotechnology* **2005**, *16*, 754–758.
- [10] S. H. Choi, B. S. Kim, C. D. Frisbie, *Science* **2008**, *320*, 1482–1486.
- [11] N. Tuccitto, V. Ferri, M. Cavazzini, S. Quici, G. Zhavnerko, A. Licciardello, M. A. Rampi, *Nat. Mater.* **2009**, *8*, 41–46.
- [12] G. J. Ashwell, P. Wierzchowiec, C. J. Bartlett, P. D. Buckle, *Chem. Commun.* **2007**, 1254–1256.
- [13] G. J. Ashwell, P. Wierzchowiec, L. J. Phillips, C. Collins, J. Gigon, B. J. Robinson, C. M. Finch, I. R. Grace, C. J. Lambert, P. D. Buckle, K. Ford, B. J. Wood, I. R. Gentle, *Phys. Chem. Chem. Phys.* **2008**, *10*, 1859–1866.
- [14] J. Tang, Y. Wang, J. E. Klare, G. S. Tulevski, S. J. Wind, C. Nuckolls, *Angew. Chem.* **2007**, *119*, 3966–3969; *Angew. Chem. Int. Ed.* **2007**, *46*, 3892–3895.
- [15] G. J. Ashwell, B. Urasinska-Wojcik, Pat. Appl. 0909244.6, **2009**.
- [16] G. Sauerbrey, *Z. Phys.* **1959**, *155*, 206–222.
- [17] J. J. W. M. Rosink, M. A. Blau, L. J. Geerligs, E. van der Drift, B. A. C. Rousseeuw, S. Radelaar, W. G. Sloof, E. J. M. Fakkeldij, *Langmuir* **2000**, *16*, 4547–4553.
- [18] G. J. Ashwell, B. Urasinska, W. D. Tyrrell, *Phys. Chem. Chem. Phys.* **2006**, *8*, 3314–3319.
- [19] M. Elbing, R. Ochs, M. Koentopp, M. Fischer, C. von Hanisch, F. Weigend, F. Evers, H. B. Weber, M. Mayor, *Proc. Natl. Acad. Sci. USA* **2005**, *102*, 8815–8820.
- [20] P. Jiang, G. M. Morales, W. You, L. P. Yu, *Angew. Chem.* **2004**, *116*, 4571–4575; *Angew. Chem. Int. Ed.* **2004**, *43*, 4471–4475.
- [21] J. W. Baldwin, R. R. Amaresh, I. R. Peterson, W. J. Shumate, M. P. Cava, M. A. Amiri, R. Hamilton, G. J. Ashwell, R. M. Metzger, *J. Phys. Chem. B* **2002**, *106*, 12158–12164.
- [22] a) R. M. Metzger, T. Xu, I. R. Peterson, *J. Phys. Chem. B* **2001**, *105*, 7280–7290; b) N. Okazaki, J. R. Sambles, M. J. Jory, G. J. Ashwell, *Appl. Phys. Lett.* **2002**, *81*, 2300–2302.
- [23] A. Honciuc, A. Jaiswal, A. Gong, H. Ashworth, C. W. Spangler, I. R. Peterson, L. R. Dalton, R. M. Metzger, *J. Phys. Chem. B* **2005**, *109*, 857–871.
- [24] a) G. J. Ashwell, D. S. Gandolfo, R. Hamilton, *J. Mater. Chem.* **2002**, *12*, 416–420; b) G. J. Ashwell, D. S. Gandolfo, *J. Mater. Chem.* **2002**, *12*, 411–415; G. J. Ashwell, D. S. Gandolfo, *J. Mater. Chem.* **2001**, *11*, 246–248.
- [25] a) G. J. Ashwell, A. Chwialkowska, L. R. H. High, *J. Mater. Chem.* **2004**, *14*, 2848–2851; G. J. Ashwell, A. Chwialkowska, L. R. H. High, *J. Mater. Chem.* **2004**, *14*, 2389–2394; b) G. J. Ashwell, R. Hamilton, L. R. H. High, *J. Mater. Chem.* **2003**, *13*, 1501–1503.
- [26] N. J. Geddes, J. R. Sambles, D. J. Jarvis, W. G. Parker, D. J. Sandman, *Appl. Phys. Lett.* **1990**, *56*, 1916–1918; N. J. Geddes, J. R. Sambles, D. J. Jarvis, W. G. Parker, D. J. Sandman, *Appl. Phys. Lett.* **1992**, *71*, 756–768.
- [27] G. Ho, J. R. Heath, M. Kondratenko, D. F. Perepichta, K. Arsenault, M. Pézolet, M. R. Bryce, *Chem. Eur. J.* **2005**, *11*, 2914–2922.
- [28] M. Brust, M. Walker, D. Bethell, D. J. Schiffrin, R. Whyman, *J. Chem. Soc. Chem. Commun.* **1994**, 801–802.